Insights into ground strike point properties in Europe through the EUCLID Lightning Location System

Dieter R. Poelman[1], Hannes Kohlmann[2], Wolfgang Schulz[2]

[1]Royal Meteorological Institute of Belgium, Brussels, Belgium
5 [2]Austrian Lightning Detection and Information System (ALDIS), Vienna, Austria

Correspondence to: Dieter R. Poelman (dieter.poelman@meteo.be)

Abstract. Evaluating the risk of lightning strikes to a particular structure typically involves adhering to the guidance outlined in IEC 62305-2. Among the multitude of factors influencing the overall risk, flash density emerges as a crucial parameter. According to its definition, each flash is assigned only one contact point to ground. Nevertheless, it is well known that, on

10 average, flashes exhibit multiple ground termination points as shown by high-speed camera observations. In this research, lightning data collected by the European Cooperation for Lightning Detection (EUCLID) network is utilized in combination with a ground strike point (GSP) algorithm that aggregates individual strokes within a flash into ground strike points. This approach enables the examination of spatio-temporal patterns of GSPs across Europe throughout a decade, spanning from 2013 to 2022. Average GSP densities exhibit variations across the European continent, mirroring the observed patterns in flash

15 densities. The highest densities are concentrated along the Adriatic Sea and the western Balkan region, reaching peak values of up to 8.5 GSPs km^{-2} yr^{-1}. The spatial distribution of the mean number of ground strike points per flash reveals a noticeable increase in the Mediterranean, Adriatic, and Baltic Sea regions compared to inland areas. Moreover, it has been determined that the average number of GSPs per flash reaches its peak between September and November. Additionally, a daily pattern is discernible, with the lowest number of GSPs per flash occurring between 12 and 18 UTC (Universal Time Coordinated). It is

20 found that 95% of the separation distances between distinct GSPs are less than 6.7 km. Lastly, it is worth noting that the presence of the Alps has an impact on GSP behaviour, resulting in lower GSP counts in comparison to the surrounding areas, along with the shortest average distances between different GSPs.

1. Introduction

In order to make informed decisions about lightning protection measures to a particular structure, it is common practice to
25 follow the guidelines set out in IEC 62305-2 (IEC 62305-2, 2010), which serves as the authoritative standard for lightning risk assessment for structures. Among the various components that influence the risk estimation, the standard puts forward the flash density, N_G, representing the number of lightning flashes per square kilometer per year, as one of the key parameters. However, by definition, the location of a flash is determined by the position of the first cloud-to-ground (CG) stroke within the flash. On the other hand, numerous studies, supported by high-speed camera observations (Rakov et al., 1994; Valine et

30   al., 2002; Saraiva et al., 2010; Poelman et al., 2021a), have provided evidence that, on average, multiple ground strike points (GSPs) exist within multiple-stroke flashes. Hence, GSP densities should be given the pivotal role in lightning studies, particularly in the context of assessing lightning-related risks. The use of GSP densities is facilitated by the existence of modern lightning location systems (LLSs) that can accurately pinpoint most, if not all, individual strokes within a lightning flash, with precision typically within a few hundred meters. Furthermore, studying variations in GSP densities over time and across

35   geographical regions aids in the development of comprehensive lightning risk maps, contributing to improved lightning protection standards and guidelines and consequently ensuring the safety of people and property.

A recent study (Poelman et al., 2021b) delved into the performance of GSP algorithms in accurately identifying ground strike points through high-speed camera observations. The latter study found that these algorithms performed well, achieving success rates of up to approximately 90% in correctly identifying stroke types within a flash, whether they create new termination

40   points or follow pre-existing channels. However, for certain applications, the accurate determination of the total number of GSPs is of greater importance. In such cases, misclassifications in stroke types may offset each other and still yield accurate results in terms of the total number of GSPs. A subsequent investigation conducted by (Poelman et al., 2023) explored the relationship between the count of GSPs obtained through a specific GSP algorithm and the number of GSPs found in various ground truth datasets. This analysis encompassed four distinct GSP algorithms and provided insights into whether a specific

45   GSP algorithm tends to overestimate or underestimate the count of ground strike points. It was revealed that each of the four GSP algorithms exhibited some degree of overestimation or underestimation regarding the GSP count per flash. However, the calculated numbers were reasonably close, i.e., within 10 %, to the values observed in ground-truth observations.

In this paper, lightning data of negative CG strokes are gathered from the European Cooperation for Lightning Detection (EUCLID) network and ingested in a ground strike point algorithm in order to analyse spatial and temporal patterns of GSPs

50   across Europe from 2013 to 2022. Section II provides a description of the LLS data and GSP algorithm employed. Section III then examines the spatio-temporal GSP characteristics within the EUCLID domain. Our findings and a summary are offered in Section IV.

2. Data and Methodology

2.1 Lightning Location System

55   The European Cooperation for Lightning Detection (EUCLID) comprises a network of more than 170 sensors distributed across the European landscape. The network is continuously evolving by upgrading older sensors to newer models and adjusting sensor placements, either by adding new sensors or relocating existing ones. As a result, the network's configuration has undergone changes in both the past and during the investigation period, i.e., 2013-2022. However, these changes are not substantial enough to significantly affect the results presented in the following sections. The current configuration at the time

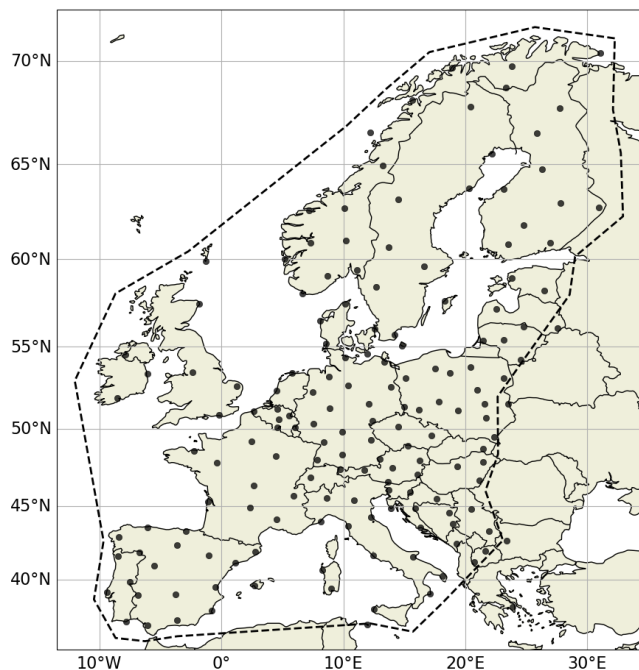60   of this writing is illustrated in Fig. 1. General information about EUCLID can be found at https://www.euclid.org.

Figure 1: Sensor locations within the EUCLID network. Only data within the dashed polygon is considered for quantitative analysis.

The network's primary function is to identify cloud-to-ground (CG) strokes and intracloud (IC) pulses by employing a combined methodology that incorporates time-of-arrival (TOA) and direction-finding (DF) techniques. The EUCLID network is continuously evaluated by assessing its performance in terms of detection efficiency (DE), location accuracy (LA), and peak current estimation. This assessment is conducted using a dual approach. On one hand, it leverages direct lightning measurements obtained from instrumented towers, and on the other hand, it utilizes video and electric field (E-field) recordings collected from various locations. Analysis of the instrumented tower data reveals that the LA achieved by EUCLID is approximately 100 meters. Moreover, the DE for negative CG strokes and flashes is found to be 70% and 96%, respectively. When video and E-field records are employed, the DE for negative CG strokes and flashes is determined to be 84% and 98%, respectively, as evidenced by previous studies (Schulz et al., 2016; Diendorfer, 2016). The stroke DE derived from tower measurements is significantly lower than when evaluating natural downward lightning. This reduction stems from the fact that tower lightning measurements only capture subsequent strokes, which, on average, exhibit lower peak currents than first strokes and are consequently harder to detect. We assume that the latter DE and LA values mentioned are applicable within the dashed polygon indicated in Fig. 1 and diminishes as you move farther away from the network's periphery. Hence, for quantitative analysis, data within this polygon, over the ten-year period from 2013 until 2022, is exclusively considered.

2.2 Ground strike point algorithm

Prior to attempting the merging of CG strokes into GSPs, it is necessary to group first individual strokes that are part of the same lightning flash. In this process, which utilizes CG observations obtained from a LLS, the creation of artificial flashes relies on well-defined and frequently employed spatial and temporal criteria. Specifically, strokes are considered part of a single flash if their time difference (Δt) is less than 1.5 s and their spatial separation (Δd) is less than 10 km, both calculated in reference to the time and position of the first stroke in the flash. Additionally, a temporal interstroke interval criterion of 0.5 s is applied. After allocating each individual stroke to their respective flashes, a GSP algorithm can be executed to group the observed CG strokes of a flash in one or more GSPs. What follows is a concise overview of the GSP algorithm that was utilized. For a more comprehensive analysis of the algorithm's performance, readers who are interested are directed to (Poelman et al., 2021b; Poelman et al. 2023), where the algorithm is denoted as A1.

The GSP algorithm employs an iterative K-means approach by sequentially examining the strokes within a flash in chronological order. The initial position of the first GSP is determined by the location of the first stroke. Subsequently, the algorithm assesses the distance between each successive stroke and the existing GSPs against a predefined threshold value; being 500 m. If this distance is less than the threshold, the stroke is assigned to the nearest GSP. However, if the distance exceeds the threshold, a new GSP is created, provided that all distances to the existing GSP locations surpass the threshold. The positions of the GSPs are updated at the end of each iteration, with each stroke being assigned a weight that is inversely proportional to its respective semi-major axis (SMA) of the error ellipse. In addition, a stroke is assigned to the previous GSP regardless its position when the absolute peak current $|I_\mathrm{p}|$ is below 6 kA and/or the SMA is larger than 2 km. The latter is carried out to prevent the formation of spurious GSPs caused by imprecisely located strokes.

The selection of a 500-meter threshold is based on several factors. Firstly, at this threshold, the GSP algorithm demonstrates its optimal performance in distinguishing stroke types, as described in Poelman et al. (2021b). Secondly, when using a 200-meter threshold, the ratio of GSPs detected by the algorithm to the GSPs observed in high-speed video recordings (as detailed in Poelman et al. 2023) was approximately 1, but at the 500-meter threshold, it only underestimates the observed GSP count by no more than 5%, based on a limited ground-truth data set taken in France, Austria and Spain. Thirdly, it's noteworthy that the median value of the semi-major axis of the 50% error ellipse within the polygon consistently remains below 500 meters in the complete region of investigation. Nevertheless, considering that some regions within the EUCLID domain exhibit a median SMA surpassing 200 m, the decision is made to employ a 500 m threshold to be on the safe side.

3. Results

3.1 Spatial characteristics

In this section, we begin by examining observations made across the EUCLID domain. Following that, a specific area, intriguing due to its geographical location and deserving a more comprehensive investigation based on the upcoming results,
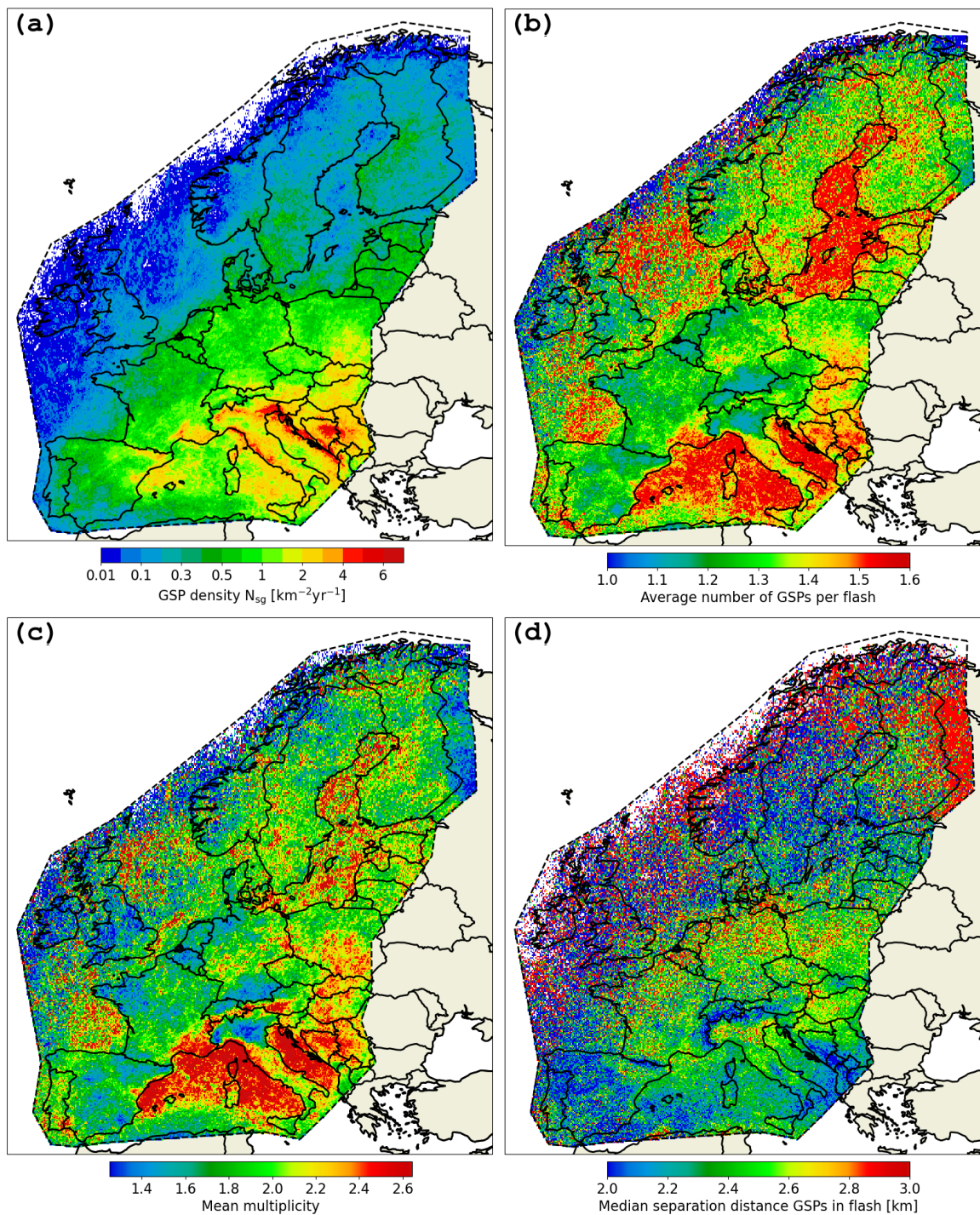
Figure 2: Spatial distribution of the (a) mean annual ground strike point density N_{sg} [km^{-2} yr^{-1}], (b) average number of GSPs per flash (GSPF), (c) mean multiplicity, and (d) median separation distance amongst GSPs in a flash.

is highlighted and explored in greater detail. The geographic plots that follow are displayed using a spatial resolution of 0.1°
x 0.1°. This grid size is adequate to meet the minimum requirements outlined in Diendorfer (2008), ensuring a spatial
110   uncertainty of less than 20% at a 90% confidence level throughout the EUCLID domain.

Figure 2a illustrates the average GSP densities across the European continent. It is expected that the observable variations in
GSP densities correspond to the flash patterns outlined in a previous study conducted by Poelman et al. (2016b), meaning that,
as a general trend, regions with higher flash densities tend to exhibit higher GSP densities. The highest concentrations are
located near the Adriatic Sea and the western Balkan region, where they can reach a maximum of 8.5 GSPs per square kilometre
115   per year.

When analysing the spatial pattern of the average number of GSPs per lightning flash (GSPF), as depicted in Figure 2b, a clear
increase is observed in the Mediterranean, Adriatic, and Baltic Sea regions in contrast to inland regions. The investigation
reveals that in the sea regions mentioned earlier, the average count of GSPF is approximately 1.5 or greater, while over land,
this value decreases to around 1.3. However, there is a simple factor influencing this situation, which can be easily understood
120   by examining Figure 2c. This figure provides a visual representation of the average multiplicity, i.e., the count of CG strokes
within a single flash. Across the entire EUCLID domain, negative flashes exhibit an average multiplicity of 2.1, with a
substantial 95% of the flashes comprising six strokes or fewer. The majority of negative CG flashes are single-stroke
occurrences, making up 58% of the recorded flashes over the EUCLID domain. However, it's crucial to emphasize that the
percentage of single stroke flashes represent an overestimation compared to values derived from ground truth recordings. It is
125   closely associated with the stroke DE, the algorithm employed for grouping strokes into flashes, and, last but not least, the
misclassification of IC pulses as CG strokes. It becomes evident that regions with higher multiplicity align with areas that
exhibit a higher number of ground strike points per lightning flash. In essence, the figures 2b and 2c complement each other
in demonstrating this relationship.

By utilizing the GSP positions within a flash, obtained through the GSP algorithm, it becomes feasible to calculate the distances
130   between the various GSPs relative to all of them within that same flash. Figure 2d displays the spatial pattern of the median
separation distance of GSPs in flashes. The median value is reported at 2.3 km, with the 10th and 90th percentiles measuring
900 meters and 5.5 km, respectively. A notable observation is the closer proximity of GSPs in a flash in the Alpine, Pyrenean,
and Apennine regions. The connection between the distance between GSPs and the overall elevation of the terrain has also
been previously noted by Cummins (2014). Cummins conducted a study on the influence of terrain on lightning occurrence in
135   two distinct areas within the United States and conclusively established a spatial correlation between the absolute elevation of
the terrain and the separation distance, particularly in the vicinity of the Rocky Mountains. This phenomenon appears to have
a valid physical explanation. Assuming a consistent height for preliminary breakdown and considering that lightning leaders
often exhibit some degree of inclination as they move from the cloud toward the ground, it follows that in mountainous regions
with higher altitudes, this would result in shorter channels and, consequently, shorter separation distances.

140   In the next part of this subsection, we focus on a particular geographical area that encompasses the Alps, Italy (including its
islands), the western Balkan region, as well as portions of the Adriatic and Mediterranean Seas. The choice of this particular
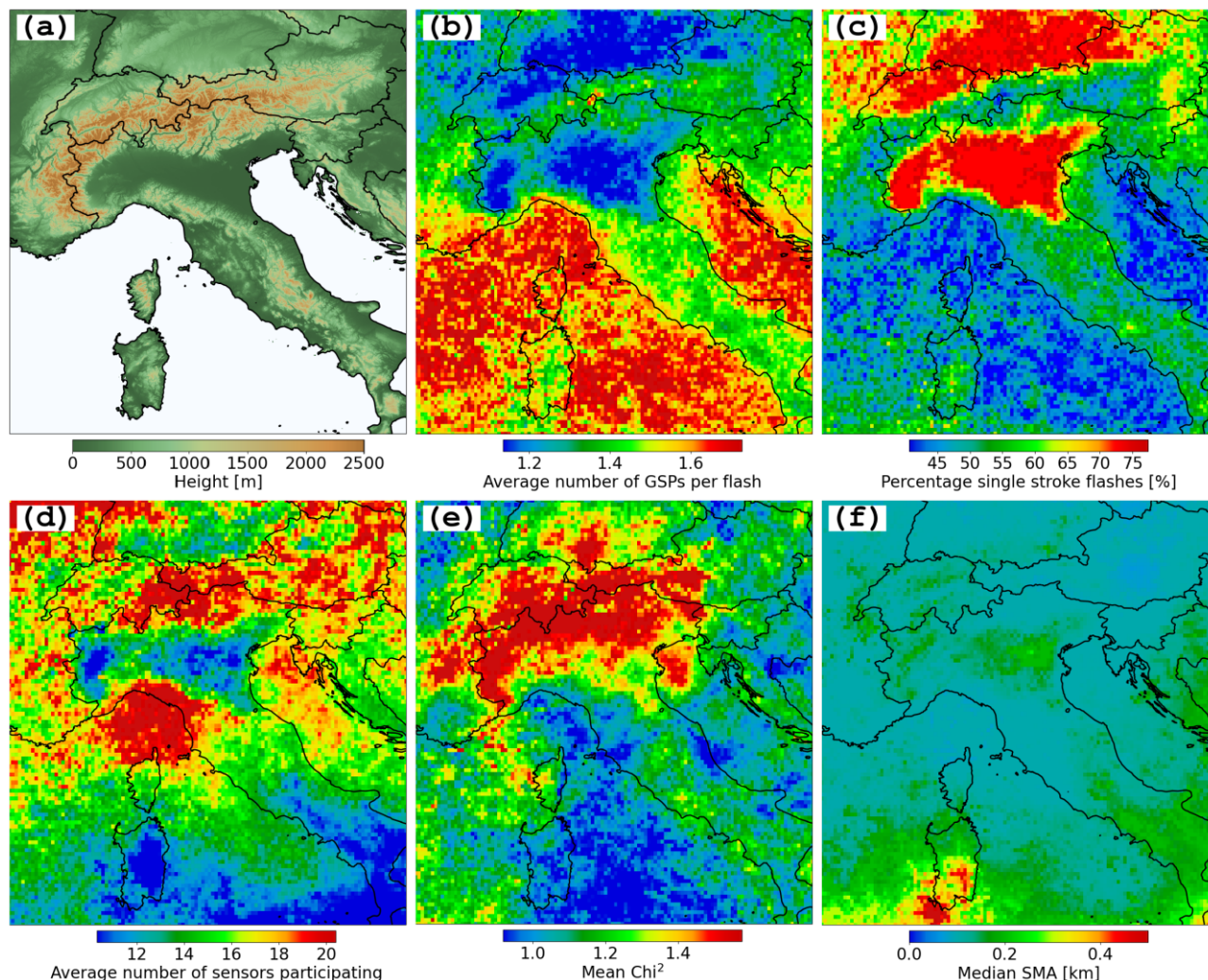
Figure 3: (a) topography, (b) average number of GSPs per flash, (c) percentage of single stroke flashes, (d) average number of sensors participating, (e) mean Chi², and (d) median length of the semi-major axis of the 50% error ellipse.

region is twofold: firstly, its diverse topography, and secondly, equally significant, it is suitable for exploring the potential differences that might be present between land and sea. To achieve this objective, Figures 3 to 5 are utilized to evaluate the potential influence of LLS performance on the outcomes and to conduct a more comprehensive examination of the observed GSP behaviour.

Figure 3a provides a representation of the topographical features in this region, showcasing the variations in altitude, notably the pronounced elevation of the Alps, and to a lesser extent, the Apennines, in comparison to their lower surrounding areas. Figure 3b displays an identical plot to that of Figure 2b, illustrating the average GSPF. It clearly highlights the contrast between land and sea, evident not only along the eastern and western coasts of Italy but also becoming apparent in the vicinity of

Sardinia. The other sub figures of Fig.3 are used to delve deeper into exploring the factors that may account for the observed disparities in the average GSPF. Noticeable differences in the proportion of single-stroke lightning flashes are apparent when comparing the regions both north and south of the Alps, as well as the Alpine region itself, as depicted in Figure 3c. Furthermore, the percentage of single-stroke flashes is at its lowest over the sea in contrast to inland areas. The geographic

155 distribution of single-stroke lightning flashes directly affects the distribution of GSPs per flash, particularly evident in the northern and southern regions of the Alps (see Fig. 3b). A similar connection is observed between the Mediterranean Sea and mainland Italy. The elevated occurrence of single-stroke flashes in the areas located to the north and south of the Alps can be attributed to the topographic influence of the Alps, which attenuates ground waves and consequently obstructs the sensors' ability to participate in locating lightning discharges. This phenomenon is primarily noted in the southern regions of the Alps,

160 as depicted in Figure 3d where the average number of sensors participating is shown. In this specific area, the average participation of sensors in a solution decreases to approximately 10 to 12 sensors. A reduction is also observed to the north of the Alps, albeit to a lesser extent than in the areas immediately to the south of the Alps. It is worth observing that in the southern regions of Italy and Sardinia, the plot depicts the lowest average participation of sensors, which is associated with a high number of sensor outages during the investigated time period. However, this discrepancy does not result in a reduced

165 proportion of single-stroke flashes when compared to what is witnessed in the northern and southern Alpine regions. Chi-square (Chi^2) values serve as an indicator of the consensus among the sensors employed for geolocating lightning discharges. In the case of a perfectly calibrated network, the average Chi^2 value is 1, while values below three are still considered satisfactory. Elevated Chi^2 values, on the other hand, are typically a result of larger arrival-time errors, which can be attributed to propagation effects. Observing Figure 3e, one can note that the most elevated Chi^2 values are situated in the Alpine region,

170 peaking at 1.5. Beyond this particular region, the average Chi^2 values are at 1.2 or lower. This suggests that, overall, the network is well-calibrated, which is especially noteworthy considering the challenging topography in the area. Furthermore, the accuracy of error ellipse parameters, particularly the semi-major axis of the 50th percentile confidence ellipse (SMA), provides additional information about the network's quality. While there are instances where median SMA values are slightly greater than in other areas, Figure 3f illustrates that, in most cases, the median SMA value remains well below approximately

175 250 meters. In summary, the collective data from Figures 3d-3f strongly suggest that the EUCLID network is effectively calibrated. Investigating the underlying reasons for the high occurrence of single stroke flashes, though intriguing, falls beyond the scope of this study. However, the reduced number of participating sensors suggests that, likely due to lower conductivity in the Alps, signals may be attenuated or distorted on the opposite side of the Alps. Therefore, this could result in lightning sensors rejecting the information either because of a lack of correlation with other sensors or when the signals are attenuated

180 to a level below the sensor threshold.

As previously demonstrated in Fig. 3b and Fig. 3c, the multiplicity distribution significantly influences the spatial pattern of the mean number of ground strike points per lightning flash. To mitigate the impact of the multiplicity distribution on the average GSPF and to genuinely explore whether flashes behave differently in terms of the production of new termination points across various topographic and conducting regions, the following method is adopted. Spatial plots are generated to
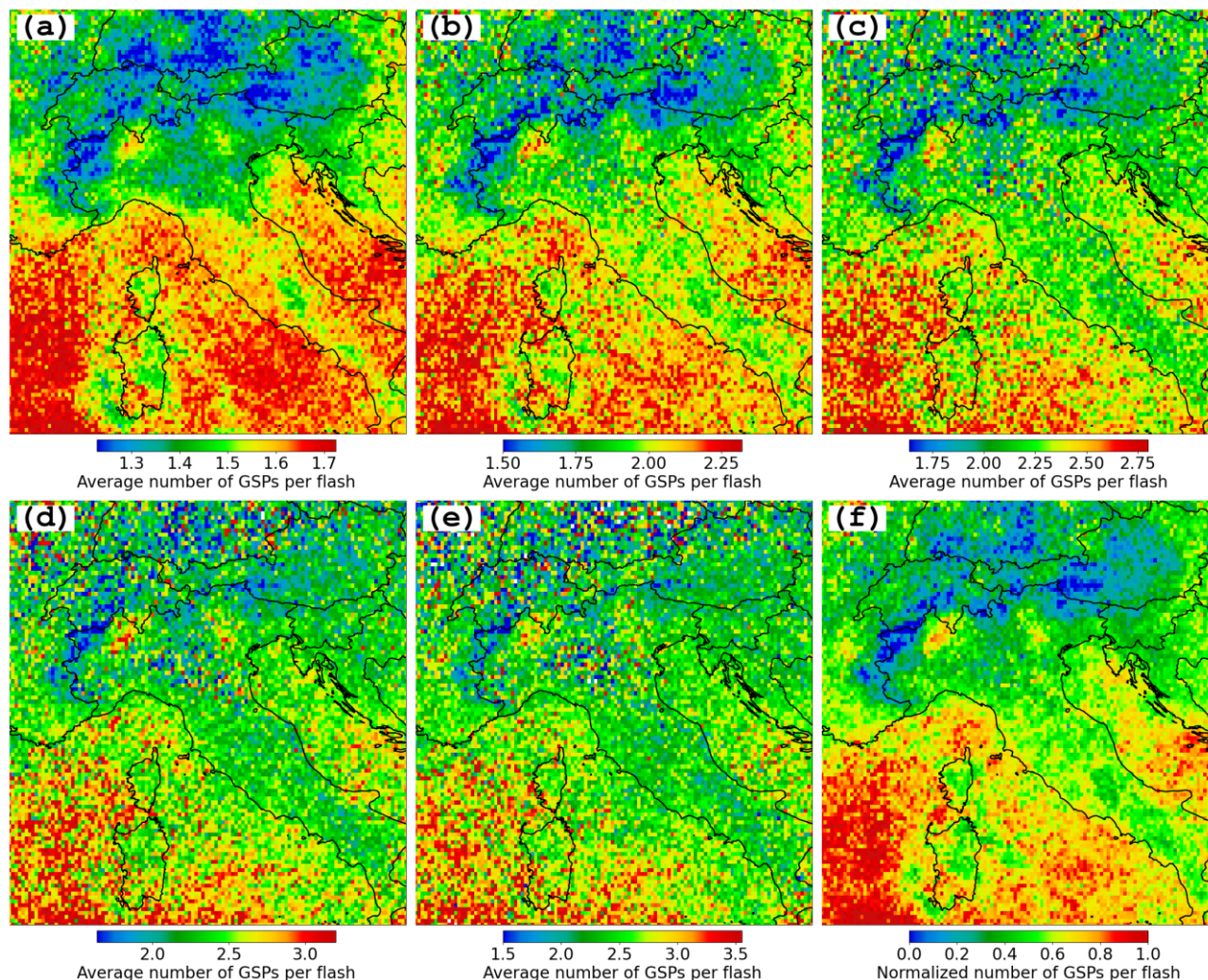
Figure 4: The mean count of ground strike points per flash for flashes having a fixed multiplicity of (a) two, (b) three, (c) four, (d) five, and (e) six. A normalized spatial distribution of these mean counts for flashes with a constant multiplicity is presented in (f).

185

illustrate the average GSPF, exclusively for flashes with particular multiplicities. This methodology enables the investigation of potential fluctuations in the average GSPF. Fig. 4 illustrates this process, presenting the mean count of ground strike points per lightning flash for flashes with fixed multiplicities ranging from 2 to 6. Two noteworthy observations emerge from this analysis. First, the average GSPF for flashes with fixed multiplicity is at its lowest over the Alps. Second, a distinct land/sea

190 disparity is evident. To alleviate the influence of multiplicity while considering flashes of all multiplicities, each of Fig. 4a–4e is scaled to values between 0 and 1. Subsequently, the spatial plots are aggregated by summing the values of the corresponding
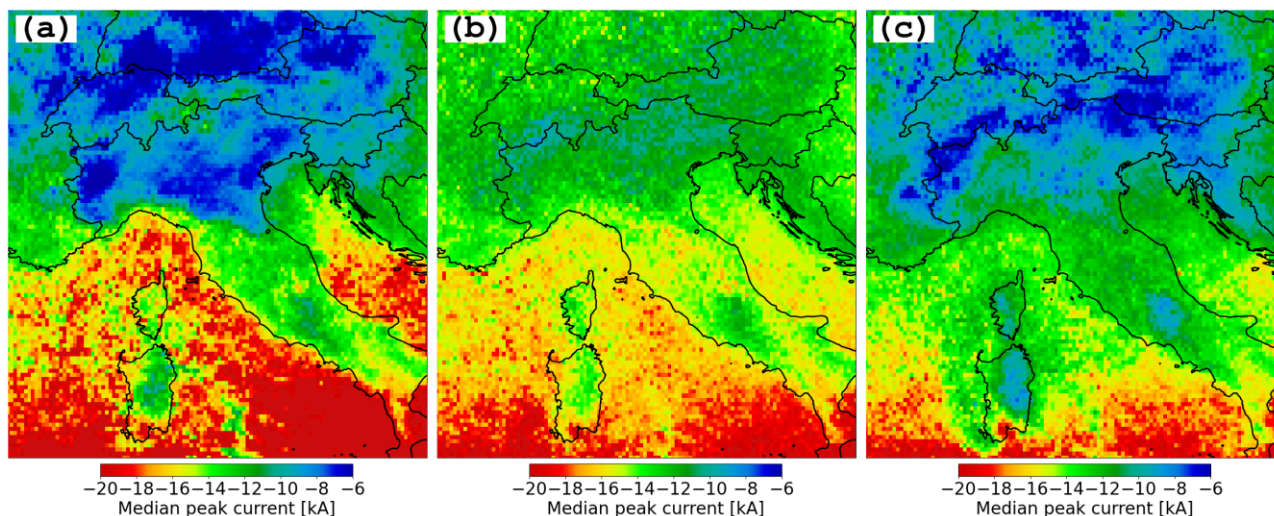
Figure 5: Spatial distribution of the median peak current amplitude for (a) flashes, (b) ground strike points excluding first strokes in a flash, and (c) subsequent strokes in ground strike points.

grid cells. The resulting composite outcome is once again normalized to ensure a scale ranging from 0 to 1. The normalized output seen in Fig. 4f provides a more accurate representation of how GSPs behave within a flash across the region.

195   The reason behind the observations in Fig. 4, in particular Fig. 4f, raises questions. An unexplored path relates to the analysis of the peak current distribution and its potential influence on the formation of new ground termination points. In previous studies it has been demonstrated that on average peak currents over sea tend to be stronger compared to the peak currents over land (Cooray et al., 2014, Nag and Cummins, 2017 Poelman et al., 2016). Cooray et al. (2014) was, to the best of the author's knowledge, the first to suggest that variations in meteorological conditions during storms underlie the distinctions observed

200   between maritime thunderclouds and those occurring over land. The conclusion drawn was that the lack or reduction of the essential prerequisites for the development of positive charge pockets below the main negative charge center within maritime clouds results in ground lightning flashes originating at a higher electrical potential within the negative charge area, in contrast to those initiated in land-based storms. Additionally, Nag and Cummins (2017 discovered that the median duration of the stepped-leader, which is the time gap between preliminary breakdown pulses and the negative first stroke, is briefer when

205   observed above the ocean compared to over land. They provided evidence that these shorter durations over the ocean correspond to the higher oceanic peak current levels that have been documented. Fig. 5 illustrates the spatial distribution of median peak current for three categories: flashes, GSPs (excluding the first strokes within a flash, which also entails the exclusion of single-stroke flashes), and the subsequent strokes within GSPs, whereby the peak current of a GSP is defined as the peak current of the initial stroke linked to that particular GSP. The flash peak currents exhibit a noticeable decrease to the

210   north and south of the Alps. This minimum arises from the high occurrence of single-stroke flashes in those regions, as we will later demonstrate that flash peak current increases with multiplicity. Consequently, this leads to the observed minimum.
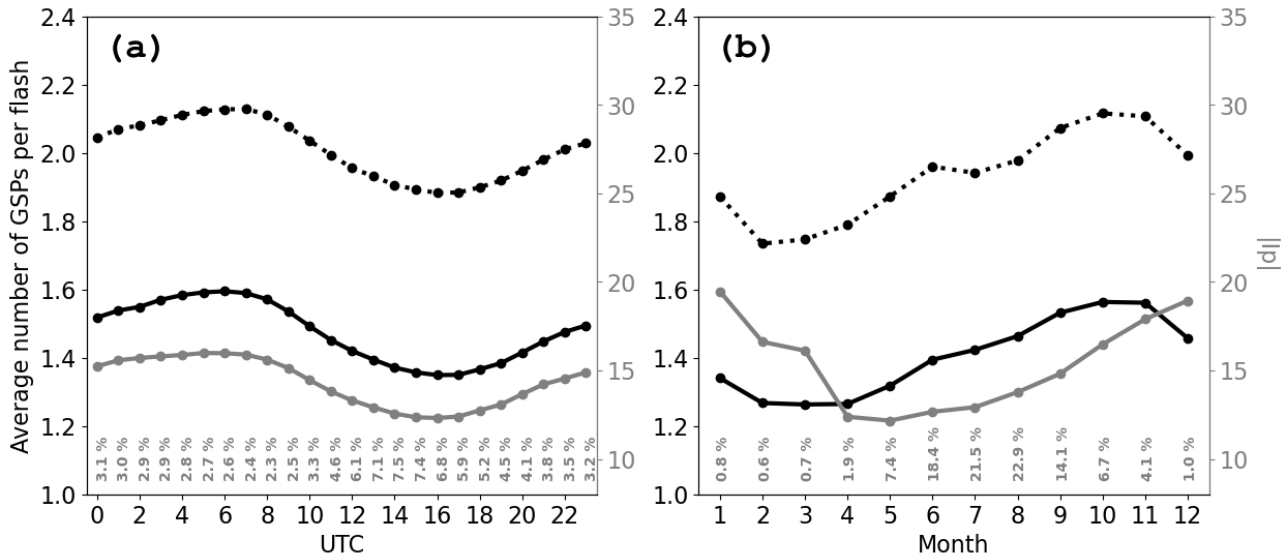
Figure 6: (a) Diurnal and (b) seasonal variation of the average number of GSPs per flash, for all flashes (solid black) and excluding single stroke flashes (dotted black). The median value of the absolute peak current is represented in grey. The numbers at the bottom indicate the proportion of activity, where 1% corresponds to approximately 700,000 strokes.

The median peak current for GSPs — excluding the first strokes within flashes — is at its lowest over the Alps, as is the case for the median values of subsequent strokes in GSPs. Per definition, the latter two categories of lightning strokes potentially contribute to the formation of new termination points or may opt to trace an existing channel. In both scenarios, the least average GSPF in the Alps coincides with the lowest observed peak current. An additional strengthening factor that could also come into play in the Alps or any mountainous terrain is that sharp peaks tend to draw lightning discharges more easily. Consequently, within a lightning flash, the probability of the discharge being drawn to the same peak, rather than establishing a new termination point at a greater distance, is enhanced. The same observation applies at the instrumented Gaisberg tower, where the multiplicity of flashes is generally higher compared to what is observed in natural cloud-to-ground lightning. Apart from the distinctions observed in the Alps, it's evident that a noticeable contrast exists between land and sea. Our findings in this study align with earlier research in that the median peak current for flashes is greater over the sea compared to over land. What's particularly noteworthy and not previously documented is that this pattern also extends to the peak current of GSPs and the subsequent strokes within GSPs as can be seen in Fig. 5b and Fig. 5c.

Additionally, this transition from land to sea conditions is evident around the regions of Sardinia and Corsica. While the conditions of the propagation path have been shown to have an impact on various lightning parameters measured by LLS
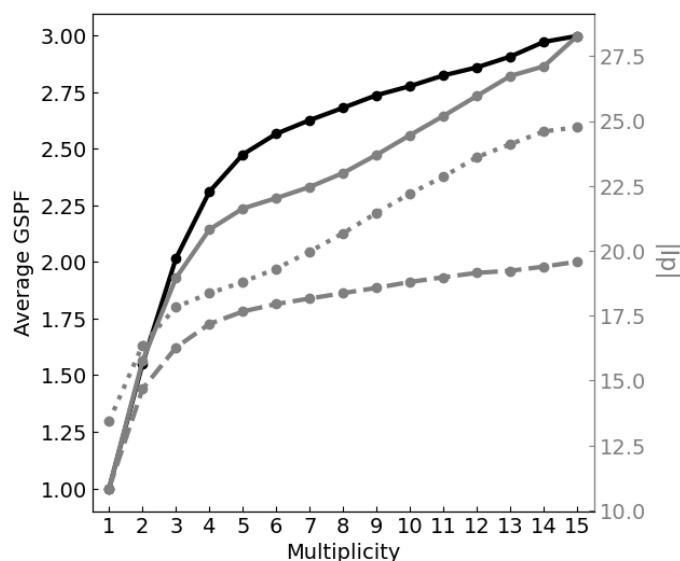
Figure 7: The graph illustrates the average number of GSPs per flash (GSPF) in relation to the flash multiplicity, depicted in black. The median absolute peak current values for flashes (solid) and for GSPs within flashes (dashed) are presented in grey, also in relation to the flash multiplicity. Additionally, the absolute median 1st stroke peak current of GSPs as a function of GSP multiplicity, i.e., the number of strokes allocated to a specific GSP, is shown (dotted).

networks (see for example Chisholm, 2017), the above results support the idea that atmospheric distinctions within thunderclouds play a primary role in the observed land-sea transition of lightning peak currents. Also in this case it is observed
230 that maritime regions exhibiting higher peak current amplitudes have a higher average GSPF. The latter implies that the observed distributions of peak current and GSPF share a common root cause. According to Nag and Cummins (2017), clouds electrified over the ocean may exhibit a larger main negative charge region and a smaller lower positive charge region. This in turn could lead to negative leaders with elevated leader tip potential and a higher line charge density, resulting in faster average vertical velocity during downward propagation. Consequently, it is probable that increased leader tip potential not
235 only leads to elevated peak currents but also concurrently raises the likelihood of branching-off instead of following a pre-existing ionized channel.

3.2 Temporal characteristics

Figure 6 depicts the fluctuations in both daily and seasonal average GSPF, alongside the peak values. As shown in Figure 6a, the highest peak current is observed during the evening to early morning hours (approximately 22-8 UTC), while it is at its
240 lowest in the afternoon. Additionally, the peak in CG lightning activity aligns with the minimum in absolute peak current. Chronis et al. (2014) previously identified this pattern and suggested that the frequent occurrence of CG lightning in convectively active conditions might hinder the accumulation of electrostatic charge within thunderclouds, leading to less

intense discharges. What is intriguing is that the distribution of the average GSPF closely mirrors the distribution of peak currents. This once more indicates that the same principles discussed in the concluding part of Sect. 3.1 are applicable in this context as well. A comparable trend can be observed in Figure 6b, but now at a monthly interval. The lowest peak current values are typically observed during the summer months, with higher values occurring at the transition between the end and start of the year. This phenomenon has been documented previously (Brook, 1992) and is thought to be linked to the observation that electric field initiation of lightning is more pronounced during winter compared to summer. Consequently, discharges occurring in winter tend to be more energetic, featuring higher peak currents. The relationship between the average GSPF and the absolute peak current is noticeable on a monthly scale, but it is not as strong as it is at the daily level.

3.3 Additional characteristics

Figure 7 presents the average GSPF in relation to the flash multiplicity. Furthermore, it features the median absolute peak current values both for flashes and for GSPs within a flash as a function of the flash multiplicity. Additionally, it illustrates the absolute median peak current of GSPs as a function of the GSP multiplicity, i.e., the number of strokes associated to a GSP. Note that the peak current of a flash corresponds to the peak current of its initial stroke, and similarly, the peak current of a GSP is determined by the peak current of the first stroke associated with that GSP. Certainly, as the flash multiplicity increases, the likelihood of generating additional termination points also grows, as is demonstrated by the black curve. GSPF exhibits a steep increase at lower multiplicity levels, while the rate of increase is levelling off at flashes of even higher multiplicity. Regarding the median peak current value in single-stroke flashes versus higher multiplicity flashes, it is observed that the peak current of the initial stroke in the flash is approximately twice as high in flashes with a multiplicity of three compared to single-stroke flashes (solid grey). A similar upward trend in flash peak current concerning flash multiplicity is also identified for the GSP peak current with respect to GSP multiplicity (depicted in dotted grey). Finally, it is observed that the median peak current of the GSPs within a flash is higher in flashes with increased multiplicity (depicted in dashed grey).

Finally, Fig. 8a presents the median peak current values of GSPs, sorted by their order of occurrence within a lightning flash, while Fig. 8b illustrates the median peak current of strokes in relation to the order within the corresponding GSP. According to Figure 8a, it can be inferred that the median peak current value for the first GSP in a flash is -14.3 kA, which corresponds to the median value when aggregating all the peak currents from flashes of various multiplicities as depicted in Figure 7. Interestingly, the peak current of the second GSP in a flash is approximately 1 kA greater than the flash peak current. This has been seen as well when comparing the spatial plots in Fig. 5a and 5b. This could appear surprising, but remember that, for example, the stroke responsible for generating the second GSP is not necessarily the second stroke in the flash. As demonstrated
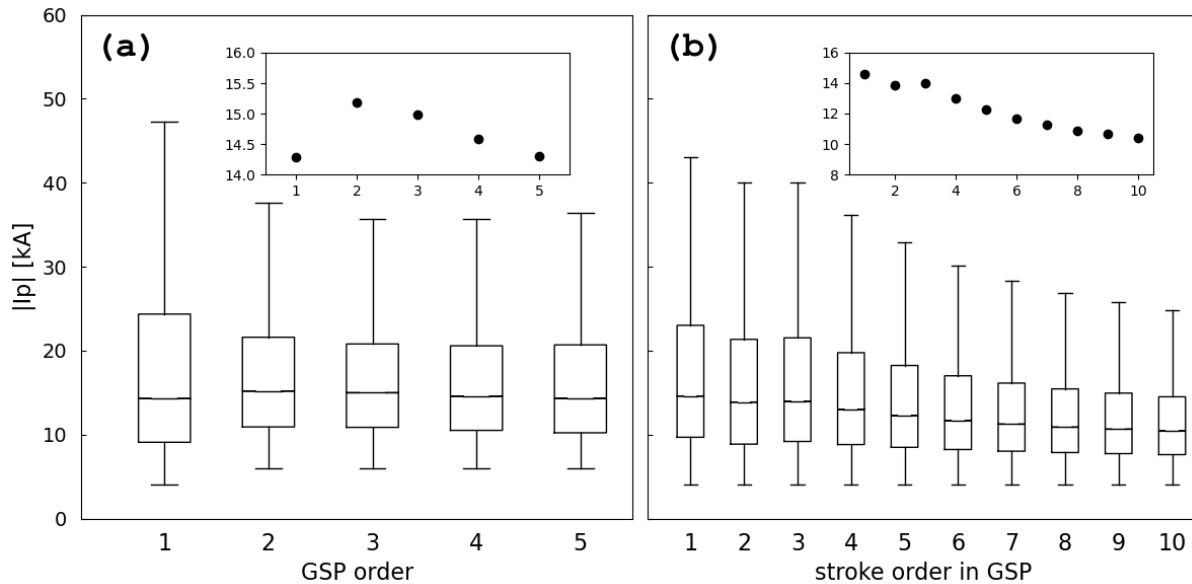
Figure 8: (a) median absolute peak current of GSP in relation to its order of occurrence within the flash, and (b) median absolute peak current of strokes as a function of stroke order within the flash.

in Figure 8b, the median peak current conforms to a more expected pattern. It shows that the first stroke within a GSP exhibits the highest peak current and gradually decreases for subsequent strokes within that GSP.

4. Summary

275   This study investigates the characteristics of ground strike points, observed through the ground-based LLS EUCLID. The investigation places emphasis on topographical impact, distinctions between land and sea areas, and how the network's performance affect the results. The spatial distribution of GSPs reveals elevated concentrations in proximity to the Adriatic Sea and the western Balkan region, closely correlating with the distribution of flash multiplicity. Nonetheless, when the influence of flash multiplicity is removed from the spatial pattern of GSPs, a distinct pattern emerges. It becomes evident that

280   the average number of ground strike points per flash is greater over sea regions in contrast to inland areas, with a minimum observed in the Alps. Furthermore, the spatial distribution of the median separation distance among GSPs within a flash clearly highlights that this value is at its lowest in mountainous regions like the Alps and the Pyrenees, displaying the significant role of terrain elevation in this context. An effort was made to explore the link between the peak current of strokes and the formation of new termination points. The study revealed that, at a daily level, the peak current variation closely aligns with the distribution

285   of GSPF, and this relationship persists at a monthly level, albeit with somewhat less strength. Additionally, it has been demonstrated that the peak current of GSPs, excluding the first strokes in a flash, as well as the subsequent strokes within GSPs, is lower over the Alpine regions and highest over the sea (see Fig. 5b and 5c), exactly corresponding to the observed

pattern in GSPF. We argue that the observed distributions of peak current and GSPF stem from a common underlying cause. Assuming the validity of the hypothesis proposed by Nag and Cummins (2017), the lack or reduction of a positive charge

290 pocket and larger main negative charge in maritime thunderclouds, results in a field configuration that leads to an enhanced leader tip potential. This sequence of effects culminates in increased peak currents and an increased likelihood of establishing a new termination point. However, the mechanism explaining how or why increased peak current leads to a higher probability for the subsequent leader to branch off remains a topic for further investigation. Ultimately, the results from this study significantly advance our understanding of lightning behaviour in Europe. Moreover, the findings have the potential to strongly

295 impact safety measures for lightning protection, particularly when prioritizing the consideration of GSP density over flash density in the risk estimation.

Competing interests

The contact author has declared that none of the authors has any competing interests.

300 **References**

Brook, M.: Breakdown of electric fields in winter storms, Res. Lett. Atmos. Elect., 12, 47-52, 1992.

Chisholm, W. A.: Can grounding affect lightning? International Symposium on Lightning Protection (XIV SIPDA), Natal, Brazil, 2nd-6th October 2017

Chronis, T., K. Cummins, R. Said, W. Koshak, E. McCaul, E. R. Williams, G. T. Stano, and M. Grant (2015), Climatological

305 diurnal variation of negative CG lightning peak current over the continental United States, J. Geophys. Res. Atmos., 120, 582-589, doi:10.1002/2014JD022547

Cooray, V., Jayaratne, R., Cummins, K. L.: On the peak amplitude of lightning return stroke currents striking the sea, Atmospheric Research, 149 (2014), 372-376

Cummins, K. L.: Mapping the impact of terrain on lightning incidence and multiple ground contacts in cloud-to-ground flashes,

310 XV International conference on Atmospheric Electricity, 15-20 June 2014, Norman, Oklahoma, U.S.A.

Diendorfer, 2008: Some comments on the achievable accuracy of local ground flash density values. Proc. 29th Int. Conf. on Lightning Protection, Uppsala, Sweden, 6pp.

Diendorfer, G.: A review of 25 years of lightning research in Austria from 1991–2015, in: World meeting on Lightning, 6–8 April 2016, Cartagena, Colombia, 2016.

315 IEC 62305-2 (2010) Protection against lightning – Part 2: risk management.

Nag, A., and Cummins, K. L. (2017): Negative first stroke leader characteristics in cloud-to-ground lightning over land and ocean, Geophys. Res. Lett., 44, 1973-1980, doi:10.1002/2016GL072270

Poelman, D. R., Schulz, W., Diendorfer, G., and Bernardi, M.: The European lightning location system EUCLID – Part 2: Observations, *Nat. Hazards Earth Syst. Sci.*, 16, 607-616, doi:10.5194/nhess-16-607-2016, 2016.

320   Poelman, D. R., Schulz, W., Pedeboy, S., Hill, D., Saba, M., Hunt, H., Schwalt, L., Vergeiner, C., Mata, C. T., Schumann, C., and Warner, T.: Global ground strike point characteristics in negative downward lightning flashes – Part 1: Observations, Nat. Hazards Earth Syst. Sci., 21, 1909–1919, https://doi.org/10.5194/nhess-21-1909-2021, 2021a.

Poelman, D. R., Schulz, W., Pedeboy, S., Campos, L. Z. S., Matsui, M., Hill, D., Saba, M., Hunt, H..: Global ground strike point characteristics in negative downward lightning flashes – Part 2: Algorithm validation, Nat. Hazards Earth Syst. Sci., 21,

325   1921–1933, https://doi.org/10.5194/nhess-21-1921-2021, 2021b

D. R. Poelman, H. Kohlmann, W. Schulz, S. Pedeboy and L. Schwalt, "Ground strike point properties derived from observations of the European Lightning Location System EUCLID," *2023 12th Asia-Pacific International Conference on Lightning (APL)*, Langkawi, Malaysia, 2023, pp. 1-5, doi: 10.1109/APL57308.2023.10182055.

Rakov, V. A., Uman, M. A., and Thottappillil, R.: Review of lightning properties from electric field and TV observations, J.

330   Geophys. Res., 99, 10745–10750, https://doi.org/10.1029/93JD01205, 1994.

Saraiva, A. C. V., Saba, M. M. F., Pinto, O., Cummins, K. L., Krider, E. P., and Campos, L. Z. S.: A comparative study of negative cloud-to- ground lightning characteristics in São Paulo (Brazil) and Arizona (United States) based on high-speed video observations, J. Geophys. Res., 115, D11102, https://doi.org/10.1029/2009JD012604, 2010.

Schulz, W., Diendorfer, G., Pedeboy, S., and Poelman, D. R.: The European lightning location system EUCLID – Part 1:

335   Performance analysis and validation, Nat. Hazards Earth Syst. Sci., 16, 595–605, https://doi.org/10.5194/nhess-16-595-2016, 2016.

Valine, W. C. and Krider, E. P.: Statistics and characteristics of cloud-to-ground lightning with multiple ground contacts, J. Geophys. Res.-Atmos., 107, 4441, https://doi.org/10.1029/2001JD001360, 2002.